Comparative study of fast-electron-impact ionization of a hydrogen atom in circularly and linearly polarized laser fields

Gabriela Buică*

Institute of Space Science – INFLPR, Atomistilor 409, P.O. Box MG-36, 77125 Bucharest-Măgurele, Romania

(Received 27 October 2023; revised 14 March 2024; accepted 22 April 2024; published 7 May 2024)

We consider ionization of the hydrogen atom by fast electron impact in the presence of a laser field with circular or linear polarization, in the first-order Born approximation in the scattering potential. We use a semiperturbative approach in which the interaction of the laser field with the incident and outgoing electrons is treated nonperturbatively by Gordon-Volkov wave functions, while the laser-atom interaction is treated in first-order perturbation theory. Analytical expressions, in a closed form, for the direct and exchange atomic transition amplitudes are employed. A simplified formula of the total laser-assisted triple-differential cross section (TDCS) is obtained at low values of the photon energy and small momentum of the residual ion. We study the role of laser field polarization and provide a comparative analysis of TDCSs for circularly and linearly polarized laser fields as a function of polar angles of the outgoing electrons at different photon energies. An asymmetric noncoplanar scattering geometry is examined, in which the polar and azimuthal angles of the scattered electron are fixed, while the ejected electron is detected at different angles. The numerical results for TDCSs by a circularly polarized laser field are compared to those derived by a linearly polarized laser field and notable differences are found in both magnitude and angular distributions of the TDCSs.

DOI: 10.1103/PhysRevA.109.052808

I. INTRODUCTION

The ionization of atoms by electron impact, referred to as the $(e, 2e)$ process, is one of the fundamental processes in atomic physics that allows understanding of the electronic structure of the target and residual ions and collision dynamics and is of interest in other fields such as astrophysics or plasma physics which need accurate scattering cross sections [1–3]. The early $(e, 2e)$ experiments used this process as a tool [4] for measuring the momentum distribution of the ejected electrons at high kinetic energies, in coplanar symmetric scattering geometries. Many $(e, 2e)$ experiments have been performed with different target atoms and in several scattering configurations, and electron momentum spectroscopy (EMS) has been developed to provide information on the electronic structure of atoms and molecules [5–7]. Over the past 40 years the study of electron-impact ionization of an atom in the presence of a laser field [8] has attracted increasing interest. The Coulomb-Volkov wave function was first proposed by Jain and Tzoar [9] to take into consideration the influence of the Coulomb field of the nucleus on the slow ejected electron, and the effect of the Coulomb interaction in laser-assisted $(e, 2e)$ collisions on hydrogen atoms was studied in many papers by using various wave functions of the ejected electron [8,10–12]. Later on, the semiperturbative theory of Byron and Joachain [13] for laser-assisted electron-hydrogen scattering in which the atomic dressing was included in the first-order time-dependent perturbation theory (TDPT) was extended to the laser-assisted $(e, 2e)$ process in hydrogen [14], showing a strong dependence on the laser field parameters, for fast incident and scattered electrons and slow ejected electrons, in an asymmetric coplanar geometry. For a bichromatic laser field, the coherent phase control in electron-hydrogen ionizing collisions in an asymmetric coplanar scattering geometry was investigated by Milošević and Ehlotzky [15], at low photon energies with the atomic dressing described within the closure approximation. For linearly polarized (LP) and circularly polarized (CP) laser fields, Taïeb *et al.* [16] studied the influence of laser polarization on the laser-assisted $(e, 2e)$ process in hydrogen for slow ejected electrons in an asymmetric coplanar geometry and showed that a CP laser can give a significantly larger TDCS than for the LP case. Later on, Makhoute *et al.* [17] showed, for the He atom, that a CP laser can give a significantly larger TDCS than for the LP case of the laser-assisted $(e, 2e)$ process at low energies of the ejected electrons. Recently, new theoretical studies of laser-assisted EMS for ejected electrons of high energies and large momentum transfer have shown that the atomic dressing terms, obtained in the closure approximation, modify the laser-assisted triple-differential cross section (TDCS) at low photon energies in the symmetric noncoplanar EMS kinematics, for both LP and CP laser fields [18,19].

Höhr *et al.* [20,21] reported the first kinematically complete experiment for electron-impact ionization of He atoms in the presence of a $\lambda = 1064$ nm laser pulse for fast electrons of 1 keV and observed significant differences of the TDCSs in comparison to the results obtained in the absence of the laser field. More recently, Hiroi *et al.* [22] observed laser-assisted electron-impact ionization of Ar atoms and reported that the intensity of the angle integrated signal for one-photon absorption was about twice as large when compared to

*buica@spacescience.ro

previous theoretical calculations in which the atomic dressing was neglected [10,11].

The goal of the present work is to study the ionization of hydrogen by fast electron impact in the presence of a laser field in the general case of asymmetric noncoplanar scattering geometries. The laser-assisted processes have a nonlinear character, which consist in absorption (emission) of photons from (to) the laser field, and from a theoretical point of view, the H atom is the most interesting simple target and closed-form expressions for the TDCS can be derived. Another motivation of our paper is to check if the enhancement effect of the CP versus the LP laser field is still present in the case of fast projectile and ejected electrons. We investigate the role of laser field polarization on the TDCS for the laser-assisted $(e, 2e)$ process and perform a comparative analysis of TDCSs by circularly and linearly polarized laser fields. Because the laser-assisted $(e, 2e)$ process is a complex problem, a semiperturbative approach is used as described in our previous work [23], and our theoretical framework presents the following distinctive features. The interaction of a laser field with the incident and outgoing electrons is treated nonperturbatively by Gordon-Volkov wave functions [24,25], while the laser-atom interaction is treated in the first-order perturbation theory in the laser field. We consider nonrelativistic collisions in which the kinetic energies of the incident and outgoing electrons are much higher than the atomic unit and therefore we are able to use the first-order Born approximation in the electron-atom scattering potential taking into consideration the exchange effects [26,27]. The influence of the residual ion on the outgoing electrons is neglected, because the Coulomb field of the residual ion is weak compared to the laser field strength [28–30]. In order to avoid direct one- and multiphoton ionization processes, the intensity of the laser field is considered moderate, i.e., much lower than the atomic unit, $3.51 \times 10^{16}\,\mathrm{W\,cm^{-2}}$. In contrast to earlier theoretical works involving laser fields of circular polarization [16,18], the present semiperturbative approach is beyond the two-level model; it not only includes the atomic dressing effects at low photon energies, but takes into consideration the exchange effects and is valid for incoming and outgoing electrons of high energies.

The organization of the paper is the following. In Sec. II we briefly describe the theoretical approach used in the laser-assisted ionization of the H atom by fast electron collisions and introduce the analytical expressions for the transition amplitudes and TDCS. At low-photon energies, we derive a simplified analytic formula of the total TDCS in the laser-assisted $(e, 2e)$ ionization process, summed over the number of exchanged photons, which includes the atomic dressing in the lowest order in the photon energy. We also examine the factorization of the TDCS formula at low photon energies. In Sec. III we present our numerical results, where the TDCSs for laser-assisted electron impact ionization of hydrogen are analyzed as a function of the polar angles of the outgoing electrons at different photon energies. We perform a qualitative comparison with the experimental results published by Höhr *et al.* [21], for the He atom. We study the polarization effects on the angular distribution of the TDCS by comparing the CP and LP laser field contributions. The importance of the atomic dressing effects is also discussed. We investigate how the azimuthal distributions of the ejected electrons are modified by the CP and LP laser fields at different polar angles of the scattered electron. In Sec. IV we provide a summary and discuss our conclusions. Unless specified otherwise, we use atomic units (a.u.) throughout this paper.

II. THEORETICAL APPROACH

We study the ionization of the H atom by electron impact in the presence of a laser field, namely, the laser-assisted $(e, 2e)$ process

$$e^-(E_i, \mathbf{k}_i) + \mathrm{H}(1s) + N\gamma(\omega) \rightarrow e^-(E_s, \mathbf{k}_s) + e^-(E_e, \mathbf{k}_e) + \mathrm{H}^+(\mathbf{q}), \quad (1)$$

where $E_{i\,(s)}$ and $\mathbf{k}_{i\,(s)}$ are the kinetic energy and the momentum vector of the incident (scattered) projectile electron, respectively, E_e and $\mathbf{k}_e$ are the kinetic energy and the momentum vector of the ejected electron, respectively, and $\mathbf{q}$ is the recoil momentum vector of the ionized target. The N represents the net number of photons exchanged by the projectile-atom system with the laser field and ω is the photon energy [27]. The CP laser field is treated classically and within the dipole approximation is described as a monochromatic electric field

$$\boldsymbol{E}(t) = iE_0(e^{-i\omega t}\boldsymbol{\varepsilon} - e^{-i\omega t}\boldsymbol{\varepsilon}^*)/2, \quad (2)$$

where E_0 denotes the amplitude, $\boldsymbol{\varepsilon} = (\mathbf{e}_j + i\mathbf{e}_l)/\sqrt{2}$ represents the polarization vector of the CP electric field, and $\mathbf{e}_j$ and $\mathbf{e}_l$ denote unit vectors in two orthogonal directions in the polarization plane. The corresponding vector potential $\boldsymbol{A}(t) = -\int^t dt' \boldsymbol{E}(t')$ is calculated from Eq. (2) as

$$\boldsymbol{A}(t) = (E_0/\omega)[\mathbf{e}_j \cos(\omega t) + \mathbf{e}_l \sin(\omega t)]/\sqrt{2}. \quad (3)$$

A. Scattering matrix in direct and exchange channels

The calculation of the scattering amplitude is a very challenging task due to the complex three-body interaction: projectile and ejected electrons, the H atom, and the laser field. We employ a theoretical framework similar to the one developed in [23] and therefore we briefly describe the model and approximations used to calculate the TDCS. We consider fast incoming and outgoing electrons with kinetic energies much higher than the energy of a bound electron of the H atom in its first Bohr orbit. Moreover, we consider an external laser field of moderate intensity and neglect the Coulomb interaction between the fast outgoing electrons and residual ion in the wave functions of the scattered and ejected electrons [28–30]. At sufficiently high kinetic energies of the projectiles it is well established that the first-order Born approximation in the scattering potential can be employed to describe the ionization process by electron impact [14,26,27]. Briefly, we utilize a semiperturbative approach of the laser-assisted $(e, 2e)$ process which is similar to that employed by Byron and Joachain for free-free transitions [13], in which the second-order Born correction in the scattering potential is negligible in comparison with the laser-dressing effects. Since the mass of the residual ion is much larger than the electron mass, we neglect the effect of the laser field on the residual ion. We should underline that the present theoretical model differs from that of Taïeb *et al.* [16], since the fast incoming and outgoing electrons wave

functions are treated to all orders in the laser field and the atomic wave function is corrected to the first order in the laser field [31].

The incident and outgoing electrons are assumed to have sufficiently high kinetic energies such that the scattering process is well treated within the first-order Born approximation in the potential $V_d(r_0, r_1) = -1/r_0 + 1/|\mathbf{r}_1 - \mathbf{r}_0|$ for the direct scattering channel and the potential $V_{\rm ex}(r_0, r_1) = -1/r_1 + 1/|\mathbf{r}_1 - \mathbf{r}_0|$ for the exchange scattering channel, where $\mathbf{r}_0$ and $\mathbf{r}_1$ are the position vectors. In order to describe the laser-assisted $(e, 2e)$ process (1), we employ the direct and exchange scattering matrix elements [32,33], which are calculated as

$$S_d^{B_1} = -i\int_{-\infty}^{\infty} dt \int d^3\mathbf{r}_0 \int d^3\mathbf{r}_1 \chi^*_{\mathbf{k}_s}(\mathbf{r}_0, t)\chi^*_{\mathbf{k}_e}(\mathbf{r}_1, t) \times V_d(r_0, r_1)\chi_{\mathbf{k}_i}(\mathbf{r}_0, t)\Psi_{1s}(\mathbf{r}_1, t), \quad (4)$$

$$S_{\rm ex}^{B_1} = -i\int_{-\infty}^{\infty} dt \int d^3\mathbf{r}_0 \int d^3\mathbf{r}_1 \chi^*_{\mathbf{k}_s}(\mathbf{r}_1, t)\chi^*_{\mathbf{k}_e}(\mathbf{r}_0, t) \times V_{\rm ex}(r_0, r_1)\chi_{\mathbf{k}_i}(\mathbf{r}_0, t)\Psi_{1s}(\mathbf{r}_1, t), \quad (5)$$

where $\chi_{\mathbf{k}_i}$, $\chi_{\mathbf{k}_s}$, and $\chi_{\mathbf{k}_e}$ represent the wave functions of the incoming and outgoing electrons interacting with the laser field and Ψ_{1s} represents the wave function of the bound electron embedded in the laser field. At kinetic energies higher than 200 eV, it is known that the plane-wave approximation agrees well with the experimental observations in the absence of a laser field [26,34] and therefore we can take advantage of the Gordon-Volkov wave functions [9,35,36]. Hence, we describe the initial and final states of the projectile electron, as well the final state of the ejected electron interacting with the electric field [Eq. (2)] by nonrelativistic Gordon-Volkov wave functions [24,25] as

$$\chi_{\mathbf{k}}(\mathbf{r}, t) = (2\pi)^{-3/2} \exp\left(i\mathbf{k}\cdot\mathbf{r} - iE_k t - i\mathbf{k}\cdot\boldsymbol{\alpha}(t) - \frac{i}{2}\int^t dt' \mathbf{A}^2(t')\right), \quad (6)$$

where $\mathbf{r}$ and $\mathbf{k}$ represent the position and momentum vectors, respectively, and $E_k = k^2/2$ is the kinetic energy. The vector $\boldsymbol{\alpha}(t) = \int^t dt' \mathbf{A}(t')$ describes the classical quiver motion of a free electron in an external electric field, and by integrating the vector potential given by Eq. (3) we easily derive, for a CP laser field,

$$\boldsymbol{\alpha}^{\rm CP}(t) = (\alpha_0/\sqrt{2})[\mathbf{e}_j \sin(\omega t) + \mathbf{e}_l \cos(\omega t)], \quad (7)$$

and $\boldsymbol{\alpha}^{\rm LP}(t) = \alpha_0 \mathbf{e}_j \sin(\omega t)$ for a LP laser field, where $\alpha_0 = \sqrt{I}/\omega^2$ is the amplitude of oscillation and $I = E_0^2$ is the intensity of the laser field. As shown in Eq. (6), at moderate electric-field strengths the largest effect of the laser on the free electron is determined by the dimensionless parameter $k\alpha_0 = \sqrt{2E_k I}/\omega^2$, which depends on the photon and electron energies and on the laser intensity. For example, a laser intensity of 1 TW cm^{-2}, a photon energy of 1.55 eV, and an electron kinetic energy of 0.2 keV result in a value of $k\alpha_0 \simeq 6.3$, while the ponderomotive (quiver) energy acquired by the electron in the electric field, $U_p = I/4\omega^2$, is about 0.06 eV and hence it can be safely neglected compared to the photon and unbound electrons energies employed in the present paper. Obviously, both $k\alpha_0$ and U_p increase with laser intensity and decrease with photon energy. We should stress that, at small kinetic energies of the ejected electron below 50 eV [2,8,37], the Coulomb-Volkov wave functions would provide a more accurate treatment, which is beyond the scope of this paper.

The interaction of the H atom in its ground state with an electric field of moderate strength is studied within the first-order TDPT. As mentioned in the Introduction, to prevent the direct one-photon and multiphoton ionization processes we consider that the electric-field strength is weak in comparison to the atomic unit, $E_0 \ll 5.14 \times 10^9$ V cm^{-1}, i.e., E_0 is much lower than the Coulomb field strength experienced by an electron in the first Bohr orbit of hydrogen atom. Thus, an approximate solution for the wave function of an electron bound to a Coulomb potential in the presence of the electric field, the laser-dressed wave function, is expressed as

$$\Psi_{1s}(\mathbf{r}_1, t) = \left[\psi_{1s}(\mathbf{r}_1, t) + \psi^{(1)}_{1s}(\mathbf{r}_1, t)\right] \times \exp\left(-iE_1 t - \frac{i}{2}\int^t dt' \mathbf{A}^2(t')\right), \quad (8)$$

where $\mathbf{r}_1$ is the position vector, ψ_{1s} is the unperturbed wave function of a hydrogen atom in the ground state, and $\psi^{(1)}_{1s}$ is the first-order perturbative correction to the atomic wave function in the external laser field. The explicit analytical form of the first-order radiative correction $\psi^{(1)}_{1s}$ is given in [23]. For the electric field given by Eq. (2) we use the analytical formula [31,38–40] of the first-order radiative correction

$$\psi^{(1)}_{1s}(\mathbf{r}_1, t) = -\frac{\alpha_0\omega}{2}[\boldsymbol{\varepsilon}\cdot\mathbf{w}_{100}(E_1^+; \mathbf{r}_1)e^{-i\omega t} + \boldsymbol{\varepsilon}^*\cdot\mathbf{w}_{100}(E_1^-; \mathbf{r}_1)e^{i\omega t}], \quad (9)$$

where we take advantage of the linear-response vector $\mathbf{w}_{100}$ of the hydrogen atom in its ground state [31] that depends on the energies $E_1^+ = E_1 + \omega + i0$ and $E_1^- = E_1 - \omega$, which refer to one-photon absorption and emission, where $E_1 = -13.6$ eV is the energy of the H atom in the ground state.

Nevertheless, since we assume that the incoming and outgoing electrons have high kinetic energies, the calculation simplifies as we use the Gordon-Volkov wave functions, and thus closed-form expression for the scattering amplitude can be derived [23]. In order to perform the time integration we develop the oscillating part of the Gordon-Volkov wave functions occurring in the scattering matrix elements (4) as a series of the ordinary Bessel functions of the first kind J_N,

$$e^{-i\boldsymbol{\alpha}(t)\cdot\mathbf{q}} = \sum_{N=-\infty}^{+\infty} J_N(X_{\rm q})\exp[-iN(\omega t - \phi_{\rm q})], \quad (10)$$

in which $\mathbf{q} = \mathbf{k}_i - \mathbf{k}_s - \mathbf{k}_e$ represents the recoil momentum vector of the ionized target, $X_{\rm q} = \alpha_0|\boldsymbol{\varepsilon}\cdot\mathbf{q}|$ is the argument of the Bessel function, namely,

$$X_{\rm q}^{\rm CP} = (\alpha_0/\sqrt{2})[(\mathbf{e}_j\cdot\mathbf{q})^2 + (\mathbf{e}_l\cdot\mathbf{q})^2]^{1/2}, \quad (11)$$

$$X_{\rm q}^{\rm LP} = \alpha_0|\mathbf{e}_j\cdot\mathbf{q}|, \quad (12)$$

for CP and LP laser fields, and $\phi_{\rm q}$ is the dynamical phase angle of $\boldsymbol{\varepsilon}$ with respect to $\mathbf{q}$, given by $\exp(i\phi_{\rm q}) = \boldsymbol{\varepsilon}\cdot\mathbf{q}/|\boldsymbol{\varepsilon}\cdot\mathbf{q}|$.

To start with the direct scattering channel, by substituting the electronic and atomic wave functions (6) and (8) into Eq. (4) and then using Eq. (10) and performing the integration with respect to time, we obtain the direct scattering matrix for the laser-assisted $(e, 2e)$ ionization process (1),

$$S_d^{B_1} = -2\pi i \sum_{N=N_{\min}}^{+\infty} T_{N,\mathrm{d}}\delta(E_s + E_e - E_i - E_1 - N\omega)e^{iN\phi_\mathrm{q}}, \tag{13}$$

where we have factorized the dynamical phase $e^{iN\phi_\mathrm{q}}$ and the δ Dirac function that ensures energy conservation. The number of emitted photons is limited and cannot be smaller than the integer value $N_{\min} = \lceil (E_e - E_i - E_1)/\omega \rceil$. The total nonlinear transition amplitude $T_{N,\mathrm{d}}$ in the direct channel can be expressed as a sum of two terms

$$T_{N,\mathrm{d}} = T_{N,\mathrm{d}}^{(0)} + T_{N,\mathrm{d}}^{(1)}, \tag{14}$$

where $T_{N,\mathrm{d}}^{(0)}$ and $T_{N,\mathrm{d}}^{(1)}$ denote the electronic and atomic transition amplitudes for the direct ionization channel, respectively.

In what follows, we briefly describe the first term in Eq. (14), namely, the electronic transition amplitude $T_{N,\mathrm{d}}^{(0)}$ that represents the transition amplitude in which the atomic dressing is ignored and only the projectile electron contribution is included [23]. After performing the integration over the coordinates $\mathbf{r}_0$ and $\mathbf{r}_1$, the electronic transition amplitude can be written as

$$T_{N,\mathrm{d}}^{(0)} = -\frac{1}{(2\pi)^2} J_N(X_\mathrm{q}) f_{\mathrm{ion}}^{B_1}. \tag{15}$$

The scattering amplitude

$$f_{\mathrm{ion}}^{B_1} = -\frac{2}{\Delta^2}\frac{\sqrt{8}}{\pi}\left(\frac{1}{(1+q^2)^2} - \frac{1}{\left(1+k_e^2\right)^2}\right) \tag{16}$$

has a form similar to the direct scattering amplitude in the absence of a laser field, i.e., with q and Δ evaluated at $N = 0$, calculated in the first-order plane-wave Born approximation, for ionization of the H atom by electron impact [1,36]. Here Δ denotes the amplitude of the momentum transfer vector from the incident to the scattered electron $\mathbf{\Delta} = \mathbf{k}_i - \mathbf{k}_s = \mathbf{k}_e + \mathbf{q}$. The first term in large parentheses in Eq. (16), $(1+q^2)^{-2}$, gives rise to the binary encounter peak [41], which occurs at the minimum value of the residual ion momentum q, and the multiplicative factor $-2/\Delta^2$ is connected to the first-order Born amplitude corresponding to scattering by the Coulomb potential $-1/r_0$. We should underline that in the direct electronic transition amplitude (15) the polarization of the laser field is only contained in the argument of the Bessel function X_q, thus being decoupled from the scattering amplitude $f_{\mathrm{ion}}^{B_1}$. This characteristic is a consequence of employing the Gordon-Volkov wave functions for fast electrons at moderate laser intensities [8,42–45].

Now we briefly describe the other term on the right-hand side of Eq. (14), namely, the atomic transition amplitude $T_{N,\mathrm{d}}^{(1)}$. This term corresponds to the laser-assisted processes in which the H atom absorbs or emits one photon and then is subsequently ionized by electron impact and is related to the atomic dressing, i.e., the modification of the atomic state by the laser field described by the first-order radiative correction $\psi_{1s}^{(1)}$ in Eq. (9). After integrating over the projectile coordinate $\mathbf{r}_0$, the direct first-order atomic transition amplitude can be expressed as

$$T_{N,\mathrm{d}}^{(1)} = -\frac{\alpha_0\omega}{2}\big[J_{N-1}(X_\mathrm{q})\mathcal{M}_{\mathrm{at}}^{(1)}(\omega)e^{-i\phi_\mathrm{q}} + J_{N+1}(X_\mathrm{q})\mathcal{M}_{\mathrm{at}}^{(1)}(-\omega)e^{i\phi_\mathrm{q}}\big], \tag{17}$$

where one photon is absorbed (emitted) by the bound electron from (to) the laser field and the rest of the $N-1$ $(N+1)$ photons are exchanged between the projectile electrons and the laser field [23]. Here we should recall that for a CP field the exponential terms involving the dynamical phase $e^{\pm i\phi_\mathrm{q}}$ are complex numbers, while for a LP field they are equal to 1 or -1. In Eq. (17), $\mathcal{M}_{\mathrm{at}}^{(1)}(\omega)$ represents the specific first-order atomic transition matrix element which refers to one-photon absorption

$$\mathcal{M}_{\mathrm{at}}^{(1)}(\omega) = -\frac{1}{\sqrt{2^3}\pi^3\Delta^2}[\boldsymbol{\varepsilon}\cdot\hat{\mathbf{q}}\mathcal{J}_{101}(\omega, q) - \boldsymbol{\varepsilon}\cdot\hat{\mathbf{k}}_e\mathcal{J}_{101}(\omega, -k_e)], \tag{18}$$

where $\hat{\mathbf{q}}$ and $\hat{\mathbf{k}}_e$ denote unit vectors that define the direction of vectors $\mathbf{q}$ and $\mathbf{k}_e$, respectively. In order to obtain the first-order atomic transition matrix element for one-photon emission, $\mathcal{M}_{\mathrm{at}}^{(1)}(-\omega)$, the replacements are made in Eq. (18), namely, $\omega \to -\omega$ and $\boldsymbol{\varepsilon} \to \boldsymbol{\varepsilon}^*$. Here $\mathcal{J}_{101}$ represents a specific radial integral which is analytically evaluated as described in [23,46] in terms of the Appell hypergeometric functions F_1 of two variables. The first-order atomic matrix element (18) is written in a closed form that explicitly contains the dot products $\boldsymbol{\varepsilon}\cdot\hat{\mathbf{q}}$ and $\boldsymbol{\varepsilon}\cdot\hat{\mathbf{k}}_e$, which allows us to analyze the effect of the laser field polarization. We should mention that the last term on the right-hand side of both the electronic scattering amplitude and atomic matrix elements (16) and (18), respectively, occurs because of the nonorthogonality of the Gordon-Volkov wave function of the ejected electron and the H atom wave function. The general structure of the atomic matrix element (18) is also similar to other laser-assisted processes with the vectors $\mathbf{q}$ and $\mathbf{k}_e$ replaced by vectors which are specific to each particular process, such as laser-assisted scattering of electrons by hydrogen atoms [47–50], laser-assisted electron-impact excitation of hydrogen atoms [44,45,51], or laser-assisted recombination of hydrogenic atoms [52].

Because it is well known that EMS experiments [5,6] involve fast incoming and outgoing electrons with kinetic energies of comparable order of magnitude, the theoretical model includes as well the exchange effects between the scattered and ejected electrons in both the electronic and atomic contributions. As we have previously noted, the exchange scattering matrix element (5) is obtained from the direct one by interchanging the position coordinates $\mathbf{r}_1$ and $\mathbf{r}_0$ of the outgoing electrons in the direct potential and in the Gordon-Volkov wave functions $\chi_{\mathbf{k}_s}$ and $\chi_{\mathbf{k}_e}$ in Eq. (4). Thus, by using Eq. (10) and performing the integration with respect to time in Eq. (5), we obtain the exchange scattering matrix for the laser-assisted $(e, 2e)$ process in the first-order Born approximation

in the exchange potential $V_{\rm ex}$,

$$S_{\rm ex}^{B_1} = -2\pi i \sum_{N=N_{\rm min}}^{+\infty} T_{N,\rm ex}\delta(E_s + E_e - E_i - E_1 - N\omega)e^{iN\phi_{\rm q}}, \tag{19}$$

where the total nonlinear transition amplitude for the exchange channel can be written as a sum of two terms $T_{N,\rm ex} = T_{N,\rm ex}^{(0)} + T_{N,\rm ex}^{(1)}$. In what follows, we briefly present the electronic transition amplitude for the exchange channel [23]. After performing the radial integration with respect to the coordinates $\mathbf{r}_0$ and $\mathbf{r}_1$, the electronic transition amplitude in the exchange channel, in which the atomic dressing contribution is neglected, can be written as

$$T_{N,\rm ex}^{(0)} = -\frac{1}{(2\pi)^2} J_N(X_{\rm q}) g_{\rm ion,ex}^{B_1}, \tag{20}$$

where

$$g_{\rm ion,ex}^{B_1} = -\frac{2}{\Delta_e^2}\frac{\sqrt{8}}{\pi}\frac{1}{(1+q^2)^2} \tag{21}$$

is the electronic amplitude in the exchange channel for ionization of the hydrogen atom by electron impact, which agrees with the Born-Ochkur approximation [32,33,53] derived in the absence of the laser field, i.e., with q and Δ_e evaluated at $N = 0$. Here Δ_e denotes the amplitude of the momentum transfer vector from the incident to the ejected electron $\mathbf{\Delta}_e = \mathbf{k}_i - \mathbf{k}_e$. Because the electron-nucleus interaction term $-1/r_1$ in the exchange scattering potential gives zero contribution to Eq. (5), the interelectronic interaction only, $1/|\mathbf{r}_1 - \mathbf{r}_0|$, contributes to the transition amplitude in the exchange channel. Therefore, the exchange scattering amplitude $g_{\rm ion,ex}^{B_1}$ can be obtained from the direct one $f_{\rm ion}^{B_1}$ by interchanging the outgoing electrons momenta k_s and k_e and dropping the $-1/r_0$ interaction term in the direct potential.

Finally, we briefly present the first-order atomic transition amplitude for the exchange scattering channel [23]. Similarly to the direct scattering, $T_{N,\rm ex}^{(1)}$ can be written as

$$T_{N,\rm ex}^{(1)} = -\frac{\alpha_0\omega}{2}\big[J_{N-1}(X_{\rm q})\mathcal{M}_{\rm at,ex}^{(1)}(\omega)e^{-i\phi_{\rm q}} + J_{N+1}(X_{\rm q})\mathcal{M}_{\rm at,ex}^{(1)}(-\omega)e^{i\phi_{\rm q}}\big], \tag{22}$$

where $\mathcal{M}_{\rm at,ex}^{(1)}(\omega)$ represents the first-order atomic transition matrix element for the exchange scattering, which is related to one-photon absorption

$$\mathcal{M}_{\rm at,ex}^{(1)}(\omega) = -\frac{\boldsymbol{\varepsilon}\cdot\hat{\mathbf{q}}}{\sqrt{2^3}\pi^3\Delta_e^2}\mathcal{J}_{101}(\omega, q), \tag{23}$$

and $\mathcal{M}_{\rm at,ex}^{(1)}(-\omega)$ refers to one-photon emission which can be derived from Eq. (23) by making the replacements $\omega \to -\omega$ and $\boldsymbol{\varepsilon} \to \boldsymbol{\varepsilon}^*$. We should mention that for fast incident and scattered electrons with kinetic energies much higher than the atomic unit and slow ejected electrons with $E_e \ll E_s$, the electronic and atomic terms related to the exchange channel can be safely neglected in comparison to the direct channel. However, we stress that the exchange terms cannot be neglected if the momentum transfers Δ_e and Δ have comparable magnitudes.

B. Perturbative theory in the low-photon-energy approximation at $N = \pm 1$

Now it is interesting to derive some useful and simple analytical formulas for the direct and exchange atomic transition amplitudes, by retaining the lowest-order terms in the expansion of the atomic matrix elements $\mathcal{M}_{\rm at,d}^{(1)}(\omega)$ and $\mathcal{M}_{\rm at,ex}^{(1)}(\omega)$ in powers of the photon energy, which is known as the low-frequency approximation (LFA). When the photon energy is low compared to the ionization energy of the H atom $\omega \ll |E_1|$, the following approximate expression can be used in the low-photon-energy limit for the atomic radial integral [46]:

$$\mathcal{J}_{101}(\omega, p) \simeq \frac{16p}{(p^2+1)^3}\left(1 + \frac{\omega}{2}\frac{p^2+7}{p^2+1}\right). \tag{24}$$

Moreover, at small arguments of the Bessel functions $X_{\rm q} \ll 1$, i.e., in the perturbative regime of laser intensities and photon energies with $\alpha_0 \ll 1$ a.u. and/or for scattering kinematics with $|\boldsymbol{\varepsilon}\cdot\mathbf{q}| \ll 1$ a.u., it is justified to use the approximate formulas for the Bessel function [54], $J_0(X_{\rm q}) \simeq 1$ and $J_{\pm1}(X_{\rm q}) \simeq \pm X_{\rm q}/2$. Hence, for one-photon absorption ($N = 1$) and emission ($N = -1$) in the perturbative regime with $X_{\rm q} \ll 1$ and low-photon energies, by keeping the first order in laser field intensity I only in Eq. (15), we obtain a simple formula for the direct electronic transition amplitude at low momentum of the residual ion, $q \ll k_e$,

$$T_{N=\pm1,\rm d}^{(0)} \simeq \pm\frac{\sqrt{I}}{\sqrt{2}\pi^3}\frac{|\boldsymbol{\varepsilon}\cdot\mathbf{q}|}{\omega^2\Delta^2}\frac{1}{(1+q^2)^2}. \tag{25}$$

For the direct atomic transition amplitude in the low-photon-energy limit and $X_{\rm q} \ll 1$, derived from Eqs. (17) and (24), at low momentum of the residual ion $q \ll k_e$, we obtain for $N = 1$ a simplified analytical expression

$$T_{N=1,\rm d}^{(1)} \simeq \frac{\sqrt{8}}{\pi^3}\frac{\sqrt{I}}{\omega\Delta^2}\frac{|\boldsymbol{\varepsilon}\cdot\mathbf{q}|}{(1+q^2)^3}\left(1 + \frac{\omega}{2}\frac{q^2+7}{q^2+1}\right), \tag{26}$$

while $T_{N=-1,\rm d}^{(1)}$ is obtained from Eq. (26) with the replacements $\omega \to -\omega$ and $\boldsymbol{\varepsilon} \to \boldsymbol{\varepsilon}^*$.

Similarly, for the exchange scattering we derive simplified approximate expressions for the electronic and atomic transition amplitudes from Eqs. (20) and (22), at $X_{\rm q} \ll 1$ in the low-photon-energy limit, as

$$T_{N=\pm1,\rm ex}^{(0)} \simeq \pm\frac{1}{\sqrt{2}\pi^3}\frac{\sqrt{I}}{\omega^2\Delta_e^2}\frac{|\boldsymbol{\varepsilon}\cdot\mathbf{q}|}{(1+q^2)^2}, \tag{27}$$

$$T_{N=\pm1,\rm ex}^{(1)} \simeq \pm\frac{\sqrt{8}}{\pi^3}\frac{\sqrt{I}}{\omega\Delta_e^2}\frac{|\boldsymbol{\varepsilon}\cdot\mathbf{q}|}{(1+q^2)^3}\left(1 \pm \frac{\omega}{2}\frac{q^2+7}{q^2+1}\right). \tag{28}$$

In the perturbative regime at $X_{\rm q} \ll 1$ and in the low-photon-energy approximation, the electronic transition amplitudes (25) and (27) are proportional to ω^{-2}, while the atomic transition amplitudes (26) and (28) are proportional to ω^{-1}. Thus, from Eqs. (25) and (26) we can estimate the ratio of the direct atomic and electronic transition amplitudes in the limit of low photon energies, as

$$T_{N=\pm1,\rm d}^{(1)}/T_{N=\pm1,\rm d}^{(0)} \simeq \frac{4\omega}{1+q^2},$$

and a similar relation holds for the exchange scattering channel. These simple analytical formulas for the electronic and

atomic transition amplitudes involving one-photon exchange can provide more physical insight into dependence on the laser parameters of the laser-assisted $(e, 2e)$ process.

C. Nonlinear triple-differential cross section

Finally, once we have calculated the nonlinear transition probabilities we can evaluate the TDCS for the laser-assisted ionization of hydrogen by electron impact accompanied by the exchange of N photons ($N > 0$ for emission and $N < 0$ for absorption) in the first-order Born approximation in the scattering potential, by including both the direct and exchange channels. For unpolarized incident projectile and hydrogen beams and without distinguishing between the final spin states of the outgoing electrons, the TDCS [8] is defined by the expression

$$\frac{d^3\sigma_N^{B_1}}{d\Omega_s d\Omega_e dE_s} = (2\pi)^4 \frac{k_s k_e}{k_i}\left(\frac{1}{4}|T_{N,\mathrm{d}} + T_{N,\mathrm{ex}}|^2 + \frac{3}{4}|T_{N,\mathrm{d}} - T_{N,\mathrm{ex}}|^2\right), \tag{29}$$

which is averaged over the initial spin states and summed over the final spin states. The incident electrons are scattered into solid angles Ω_s and $\Omega_s + d\Omega_s$ with a kinetic energy between E_s and $E_s + dE_s$ and the ejected electrons are emitted within solid angles Ω_e and $\Omega_e + d\Omega_e$. The electronic and atomic transition amplitudes in Eq. (29) are computed from Eqs. (15) and (17) for the direct scattering channel and from Eqs. (20) and (22) for the exchange channel. As a result, the TDCS depends on the momentum vectors of the electrons $\mathbf{k}_i$, $\mathbf{k}_s$, and $\mathbf{k}_e$; on the momentum transfers q, Δ, and Δ_e; and on the following laser parameters: intensity I, photon energy ω, and polarization $\boldsymbol{\varepsilon}$. Hence, the dominant contributions to the TDCS occur in collisions involving small momentum of the residual ion, q, small momentum transfers Δ and Δ_e, and photon energies close to resonance.

In what follows, we present an easy-to-handle TDCS formula in two limiting cases of laser field parameters.

D. Total triple-differential cross section at low photon energies

In the limit of low photon energies such that $\omega \ll |E_1|$, we can take advantage of the approximation formula (24) in the TDCS and consider the lowest order in ω in Eqs. (17) and (22). Furthermore, at low momentum of the residual ion, $q \ll k_e$, we can also neglect the second terms in Eqs. (15) and (18) and therefore a simplified LFA formula [23] for the laser-assisted TDCS is obtained,

$$\frac{d^3\sigma_N^{B_1}}{d\Omega_s d\Omega_e dE_s} \simeq \frac{k_s k_e}{k_i}|J_N(X_\mathrm{q})|^2\left(1 + \frac{4N\omega}{1+q^2}\right)^2 \times \left|\psi_{1s}^{(0)}(q)\right|^2\left(\frac{d\sigma}{d\Omega_e}\right)_{ee}, \tag{30}$$

where the recurrence relation $J_{N+1}(X_\mathrm{q}) + J_{N-1}(X_\mathrm{q}) = (2N/X_\mathrm{q})J_N(X_\mathrm{q})$ of the Bessel functions [54] was used. The foregoing LFA expression can be readily compared with that previously calculated for laser-assisted EMS in the low-photon-energy approximation by Bulychev *et al.*, namely, Eqs. (10) and (11) in [19]. Thus, the TDCS in Eq. (30) is simply expressed as a product of four terms: the squared modulus of the Bessel function of argument $X_\mathrm{q} = \sqrt{I}|\boldsymbol{\varepsilon}\cdot\mathbf{q}|/\omega^2$ and a dynamical LFA correction factor $[1 + 4N\omega/(1+q^2)]^2$, both factors depending on the laser field parameters and the momentum of the residual ion $|\psi_{1s}^{(0)}(q)|^2 = 8\pi^{-2}(1+q^2)^{-4}$, which is the squared wave function in the momentum space of the H atom in the ground state [1], and

$$\left(\frac{d\sigma}{d\Omega_e}\right)_{ee} = \frac{4}{\Delta^4}\left(1 - \frac{\Delta^2}{\Delta_e^2} + \frac{\Delta^4}{\Delta_e^4}\right), \tag{31}$$

which is the half-off-shell Mott scattering TDCS for fast projectile and outgoing electrons, which includes the exchange terms [6,32,33] and depends on the direct and exchange momentum transfers Δ and Δ_e only. We recall that the half-off-shell Mott scattering TDCS (31) is calculated in the literature [6] as $(2\pi)^4 f_{ee}^{B_1}$, in which $f_{ee}^{B_1}$ is the electron-electron collision factor calculated in the first-order Born approximation.

From Eq. (30) the total TDCS is obtained as a sum over the number of exchanged photons

$$\frac{d^3\sigma^{B_1}}{d\Omega_s d\Omega_e dE_s} = \sum_{N=N_{\min}}^{+\infty} \frac{d^3\sigma_N^{B_1}}{d\Omega_s d\Omega_e dE_s}, \tag{32}$$

and using the summation formulas of the Bessel functions [52,54] of the first kind

$$\sum_{N=-\infty}^{+\infty} J_N^2(X_\mathrm{q}) = 1, \qquad \sum_{N=-\infty}^{+\infty} N^2 J_N^2(X_\mathrm{q}) = X_\mathrm{q}^2/2 \tag{33}$$

and

$$\sum_{N=-\infty}^{+\infty} N J_N^2(X_\mathrm{q}) = 0, \tag{34}$$

we obtain a simplified formula in the LFA, at $\omega \ll |E_1|$ and $q \ll k_e$, as

$$\frac{d^3\sigma^{B_1}}{d\Omega_s d\Omega_e dE_s} \simeq \frac{k_s k_e}{k_i}\left|\psi_{1s}^{(0)}(q)\right|^2\left(\frac{d\sigma}{d\Omega_e}\right)_{ee}\left(1 + \frac{8I}{\omega^2}\frac{|\boldsymbol{\varepsilon}\cdot\mathbf{q}|^2}{(1+q^2)^2}\right). \tag{35}$$

This TDCS expression allows us to investigate the limits of validity of the Kroll-Watson-type sum-rule formula and could be practical for other approximate calculations. It shows that the total TDCS is not enhanced by the presence of the laser field for laser parameters such that $I/\omega^2 < 0.125$, neither at large values of the recoil momentum q nor for scattering geometries such that $\boldsymbol{\varepsilon}\cdot\mathbf{q} \simeq 0$. Thus, the ratio of the total TDCS by CP and LP laser fields around the minimum of q is simply given by $|\boldsymbol{\varepsilon}_{\mathrm{CP}}\cdot\mathbf{q}|^2/|\boldsymbol{\varepsilon}_{\mathrm{LP}}\cdot\mathbf{q}|^2$.

E. Total triple-differential cross section at low photon energies and weak laser fields

The other limiting case is the low-photon energies and weak laser fields such that $\alpha_0\omega \ll 1$ a.u., the so-called soft-photon approximation (SFA), in which we can neglect the laser-atom interactions $T_{N,\mathrm{d}}^{(1)}$ and $T_{N,\mathrm{ex}}^{(1)}$ in Eq. (29), and at low

momentum of the residual ion $q \ll k_e$ we obtain a simple expression of the laser-assisted nonlinear TDCS for N-photon exchange,

$$\frac{d^3\sigma_N^{B_1}}{d\Omega_s d\Omega_e dE_s} \simeq \frac{k_s k_e}{k_i} |J_N(X_q)|^2 \left|\psi_{1s}^{(0)}(q)\right|^2 \left(\frac{d\sigma}{d\Omega_e}\right)_{ee}, \quad (36)$$

as well for the total TDCS summed over the number of exchanged photons,

$$\frac{d^3\sigma^{B_1}}{d\Omega_s d\Omega_e dE_s} \simeq \frac{k_s k_e}{k_i} \left|\psi_{1s}^{(0)}(q)\right|^2 \left(\frac{d\sigma}{d\Omega_e}\right)_{ee}. \quad (37)$$

In contrast to Eq. (35), the expression (37) is independent of the laser polarization.

The foregoing formula (36) is in agreement with the TDCS given by Kouzakov *et al.* in Eq. (26) in [18], in which the atomic dressing is neglected, and obeys a Kroll-Watson-type sum rule formula (37), similar to the laser-assisted electron-atom scattering process [55]. Therefore, for an N-photon process in both the LFA and SFA, the ratio of the TDCSs by CP and LP laser fields is derived from Eq. (30) or (36) as

$$\left(\frac{d^3\sigma_N^{B_1}}{d\Omega_s d\Omega_e dE_s}\right)_{\rm CP} \left(\frac{d^3\sigma_N^{B_1}}{d\Omega_s d\Omega_e dE_s}\right)_{\rm LP}^{-1} \simeq \left|J_N\left(X_q^{\rm CP}\right)\right|^2 / \left|J_N\left(X_q^{\rm LP}\right)\right|^2. \quad (38)$$

Additionally, in the perturbative domain with $X_q \ll 1$, by using the approximate formula for the Bessel function at small arguments, $J_N(X_q) \simeq X_q^N/2^N N!$, the foregoing nonlinear TDCS ratio by CP and LP laser fields simply reads $(X_q^{\rm CP}/X_q^{\rm LP})^{2|N|}$ and depends on the scattering geometry.

III. RESULTS AND DISCUSSION

In this section we numerically evaluate our semiperturbative formulas to investigate the TDCSs given by Eq. (29), in the first-order Born approximation in the scattering potential, for electron-impact ionizing collisions in hydrogen in the presence of a CP laser field. The numerical results obtained for TDSCs for a CP laser field are compared with those obtained by a LP laser field for different scattering configurations geometries. We recall that the field-free TDCS in the $(e, 2e)$ collisions provides valuable information about the collision dynamics [6] and electronic structure of the target and can be used to obtain the electron momentum density distribution, which was first demonstrated for the hydrogen and helium atoms [1,34]. Additionally, the theoretical results of the laser-assisted TDCS can provide more useful insights for further experimental observation or theoretical studies, allowing the control and manipulation of the $(e, 2e)$ process through the laser parameters: photon energy, polarization, and intensity.

A. Scattering geometry

We start with some useful kinematic considerations in order to analyze the analytical formulas derived in the previous section. We consider the laser-assisted $(e, 2e)$ process in the general case of noncoplanar scattering geometry, as plotted in Fig. 1, in which the momentum vector of the incident electron, $\mathbf{k}_i$, defines the z axis with $\theta_i = 0^\circ$

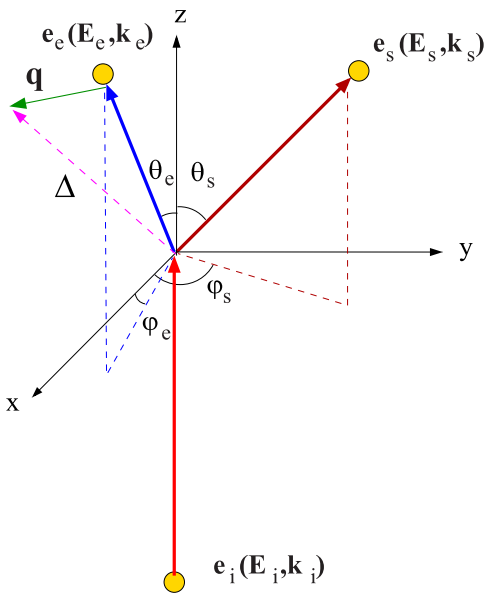

FIG. 1. Scattering geometry for the electron-impact ionization of the hydrogen atom in a laser field. The incident electron has energy E_i and momentum $\mathbf{k}_i$ with $\theta_i = 0^\circ$, while the scattered electron has energy E_s and momentum $\mathbf{k}_s$ and is detected at fixed polar angle θ_s and azimuthal angle φ_s. The ejected electron has energy E_e and momentum $\mathbf{k}_e$, and the detection polar angle θ_e and azimuthal angle φ_e are varied. Here $\mathbf{\Delta} = \mathbf{k}_i - \mathbf{k}_s$ represents the momentum transfer vector and $\mathbf{q} = \mathbf{\Delta} - \mathbf{k}_e$ is the recoil momentum vector.

and $\varphi_i = 0^\circ$. The momenta of the two outgoing electrons, $\mathbf{k}_s$ and $\mathbf{k}_e$, lie in different planes and the electrons are detected at the polar angles θ_s and θ_e, with the corresponding azimuthal angles φ_s and φ_e. Hence, the Cartesian components of the momentum vector of the residual ion, $\mathbf{q}$, are expressed as $(-k_s \sin\theta_s \cos\varphi_s - k_e \sin\theta_e \cos\varphi_e, -k_s \sin\theta_s \sin\varphi_s - k_e \sin\theta_e \sin\varphi_e, k_i - k_s \cos\theta_s - k_e \cos\theta_e)$. We consider fast incoming and outgoing electrons and investigate the asymmetric scattering geometry in which the outgoing electrons move asymmetrically with respect to the direction of the incident electron with different polar and azimuthal angles and different kinetic energies $k_s \neq k_e$. The momentum transfer of the projectile is calculated as $\Delta = (k_i^2 + k_s^2 - 2k_i k_s \cos\theta_s)^{1/2}$, while the amplitude of the momentum transfer vector $\mathbf{\Delta}_e$ is given by $\Delta_e = (k_i^2 + k_e^2 - 2k_i k_e \cos\theta_e)^{1/2}$. From the energy conservation condition the final momentum of the projectile depends on the number of exchanged photons and the photon energy $k_s = (k_i^2 - k_e^2 + 2E_1 + 2N\omega)^{1/2}$. Thus, in the asymmetric noncoplanar scattering geometry, the amplitude of the ion recoil momentum vector $\mathbf{q}$ is calculated as

$$q = \left[\Delta^2 + \Delta_e^2 - k_i^2 + 2k_s k_e \cos\theta_s \cos\theta_e + 2k_s k_e \sin\theta_s \sin\theta_e \cos(\varphi_s - \varphi_e)\right]^{1/2} \quad (39)$$

and depends on the polar angles θ_s and θ_e and on the difference between the azimuthal angles $\varphi_s - \varphi_e$ of the outgoing electrons. We may note that the symmetry relations are satisfied by the momentum of the residual ion [Eq. (39)] with respect to the polar angles of the scattered and ejected electrons $q(\theta_e, \theta_s) = q(-\theta_e, -\theta_s)$ and with respect to the

polar and azimuthal angles of the ejected electrons $q(\theta_e, \varphi_e) = q(-\theta_e, \pi + \varphi_e)$. We recall that the binary encounter peak of the TDCS occurs at the minimum value of the residual ion momentum, i.e., when $\mathbf{k}_i = \mathbf{k}_s + \mathbf{k}_e$.

B. Circularly polarized laser field

We assume that the laser beam is CP in the (x, y) plane with a polarization vector $\boldsymbol{\varepsilon}_{\rm CP} = (\mathbf{e}_x + i\mathbf{e}_y)/\sqrt{2}$ and it propagates along the z axis, which implies that

$$\boldsymbol{\varepsilon}_{\rm CP} \cdot \mathbf{q} = -(k_s \sin\theta_s e^{i\varphi_s} + k_e \sin\theta_e e^{i\varphi_e})/\sqrt{2}, \quad (40)$$

$$\boldsymbol{\varepsilon}_{\rm CP} \cdot \mathbf{k}_e = k_e \sin\theta_e e^{i\varphi_e}/\sqrt{2}. \quad (41)$$

The foregoing scalar products are invariant to the simultaneous change of $\theta_e \to -\theta_e$ and $\varphi_e \to \pi + \varphi_e$. In the particular case of forward and backward polar angles $\theta_{e\,(s)} = 0^\circ$ and 180°, respectively, the scalar products $\boldsymbol{\varepsilon}_{\rm CP} \cdot \mathbf{q}$ and $\boldsymbol{\varepsilon}_{\rm CP} \cdot \mathbf{k}_e$ cancel out and do not depend on the azimuthal angles. Hence, for a noncoplanar scattering geometry the argument of the Bessel function, for the CP laser field, is expressed as

$$X_{\rm q}^{\rm CP} = \alpha_0 \big[k_s^2 \sin^2\theta_s + k_e^2 \sin^2\theta_e + 2k_s k_e \sin\theta_s \sin\theta_e \cos(\varphi_s - \varphi_e)\big]^{1/2}/\sqrt{2}. \quad (42)$$

C. Linearly polarized laser field

We compare the numerical results for the CP laser field with those obtained for a LP laser field in which the polarization vector defines the z axis, $\boldsymbol{\varepsilon}_{\rm LP} = \mathbf{e}_z$, and therefore

$$\boldsymbol{\varepsilon}_{\rm LP} \cdot \mathbf{q} = k_i - k_s \cos\theta_s - k_e \cos\theta_e, \quad (43)$$

$$\boldsymbol{\varepsilon}_{\rm LP} \cdot \mathbf{k}_e = k_e \sin\theta_e. \quad (44)$$

Thus, for the LP laser field the argument $X_{\rm q}$ of the Bessel function simplifies to $X_{\rm q}^{\rm LP} = \alpha_0 |k_i - k_s \cos\theta_s - k_e \cos\theta_e|$.

Clearly, the condition $\boldsymbol{\varepsilon} \cdot \mathbf{q} = 0$ is fulfilled at different polar angles for the CP field than for the LP laser field. In the coplanar geometry $\varphi_s = \varphi_e$, the ratio of the argument of the Bessel function for CP and LP laser fields simply reads

$$\frac{X_{\rm q}^{\rm CP}}{X_{\rm q}^{\rm LP}} = \frac{1}{\sqrt{2}} \frac{|k_s \sin\theta_s + k_e \sin\theta_e|}{|k_i - k_s \cos\theta_s - k_e \cos\theta_e|}. \quad (45)$$

D. Numerical examples

We present in Fig. 2 a qualitative comparison with the experimental results published by Höhr *et al.* [21] for laser-assisted electron-impact ionization of the He atoms by a Nd:YAG laser of intensity $I = 4\,\mathrm{TW\,cm^{-2}}$ and $\omega = 1.17$ eV, for fast incident electrons with energy $E_i = 1$ keV. An important disagreement with the theoretical model for He was found [20,21] by comparing the differences of the TDCSs with and without a laser field, namely, the magnitude of the binary peaks is reasonable described by the theoretical model but differences between the laser-assisted (LA) and field-free (FF) TDCSs show opposite behavior to the experimental results. The authors suggested that this deviation may be related to the dressing effects of the initial atomic state, which were not included in the theoretical model [20]. Because we have not included the Coulomb correction in the ejected electron wave function, we have considered in comparison electrons emitted with the energies and polar angles $E_e = 18$ eV and $\theta_s = 8^\circ$ in Figs. 2(a) and 2(b) and $E_e = 15$ eV and $\theta_s = 5^\circ$ in Figs. 2(c) and 2(d), and the corresponding magnitudes of the momentum transfer $\boldsymbol{\Delta} = \mathbf{k}_i - \mathbf{k}_s$ (i.e., $\mathbf{q}$ in [21]) are 0.6 and 1 a.u., respectively. Our chosen parameters correspond to Figs. 4(dI), 4(dII), 4(fI), and 4(fII) in the experimental paper [21]. The solid lines in Figs. 2(a) and 2(c) represent the TDCSs, Eq. (29) summed up to $N = 10$ photon exchange (absorption and emission), while the dashed lines are the field-free TDCSs. The angular shape of TDCSs for the H atom looks similar to the one for He in Figs. 4(dI) and 4(fI) of [21], but obviously with different magnitudes, showing that the kinematical dependence is essential in the $(e, 2e)$ process. Our numerical results for the H atom in Figs. 2(b) and 2(d) show a similar behavior to the experimental results for He, namely,

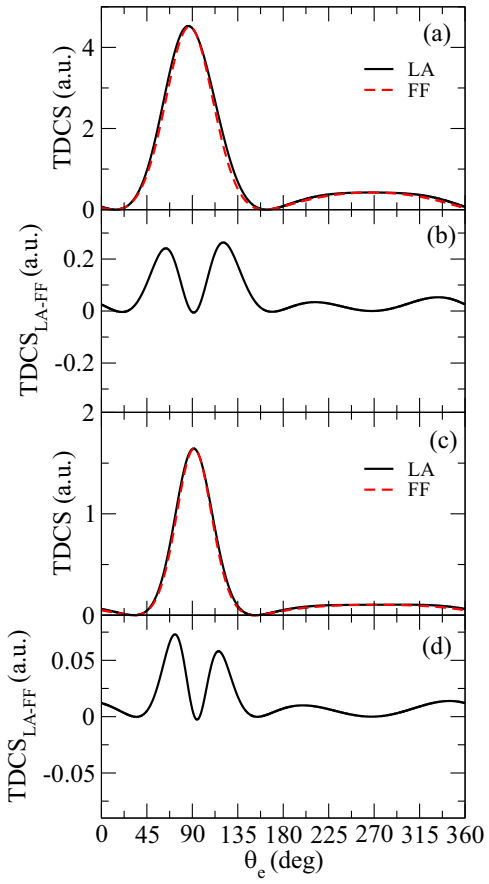

FIG. 2. (a) and (c) Comparison of TDCSs for ionization of the H atom by electron impact in the presence of a laser field (solid lines) and the field-free results (dashed lines) as a function of the polar angle of the ejected electron, for ten-photon exchange. (b) and (d) Difference between the laser-assisted (LA) and the field-free (FF) TDCSs plotted in (a) and (c), respectively. The laser field is LP along the z axis with intensity $I = 4\,\mathrm{TW\,cm^{-2}}$ and the photon energy is $\omega = 1.17$ eV. The incident electron has energy $E_i = 1$ keV and $\theta_i = 12^\circ$, while the ejected electron is emitted with energy $E_e = 18$ eV and $\theta_s = 8^\circ$ in (a) and (b) and $E_e = 15$ eV and $\theta_s = 5^\circ$ in (c) and (d), respectively. The corresponding magnitudes of the momentum transfer $\boldsymbol{\Delta} = \mathbf{k}_i - \mathbf{k}_s$ are (a) and (b) 0.6 a.u. and (c) and (d) 1 a.u.

there is an enhancement of the TDCS by the laser field and the LA and FF differences of TDCSs show an oscillatory behavior with θ_e, in qualitative agreement with the experimental results presented in Figs. 4(dII) and 4(fII) of [21]. Since the laser intensity is relatively high corresponding to a quiver motion amplitude $\alpha_0 = 5.77$ a.u. at $\omega = 1.17$ eV, the TDCS enhancement in Figs. 2(b) and 2(d) is strongly related to the interaction of the ejected electron with both the laser field and target potential as well the laser-target interaction before and after collision, as it was suggested in [21]. However, if we look at Fig. 4 of [21] to see the relative enhancement normalized to the FF TDCS, the laser dressing effect is much larger for He than for the H atom, which suggests other corrections should be included in the theoretical description. As we have mentioned, in the present numerical calculations we consider high kinetic energies of the projectile and ejected electrons $E_i = 2$ keV and $E_e = 0.2$ keV, photon energies below the ionization threshold of the H atom $\omega < |E_1|$, and a moderate laser intensity $I = 1\,\mathrm{TW\,cm^{-2}}$, which corresponds to an electric-field strength of $2.7 \times 10^7\,\mathrm{V\,cm^{-1}}$.

We now turn to the coplanar case in order to show the correlation in the TDCS between the polar angles of the outgoing electrons. Thus, in Figs. 3(a)–3(c) we present the TDCSs for a CP laser field and one-photon exchange, $N = 1$, as a function of the polar angles of the scattered and ejected electrons θ_s and θ_e, respectively, at the azimuthal angles $\varphi_s = \varphi_e = 0^\circ$ and at the following photon energies: 1.55 eV in Fig. 3(a), 4.65 eV in Fig. 3(b), and 9.3 eV in Fig. 3(c). For comparison, in Figs. 3(d)–3(f) we show similar results of the laser-assisted TDCSs as in Figs. 3(a)–3(c), but for a LP field.

Due to Coulomb repulsion, the electrons are predominantly emitted and scattered with a high probability in different half planes, corresponding to polar angles θ_s and θ_e of opposite signs with respect to the incoming electron beam. The TDCSs values in Fig. 3 are concentrated in a narrow angular range of $60^\circ \leqslant \theta_e \leqslant 90^\circ$ and $-19^\circ \leqslant \theta_s \leqslant -14^\circ$ and are invariant with respect to the simultaneous transformations $\theta_e \to -\theta_e$ and $\theta_s \to -\theta_s$. The maximum values of TDCSs occur at specific combinations of polar angles θ_e and θ_s, which are determined by the minimum value of recoil momentum q given by Eq. (39). It is worth pointing out that these binary peaks of TDCSs are split differently in the presence of the CP and LP laser fields, due to the zeros of the argument of the Bessel functions, i.e., whenever $\boldsymbol{\varepsilon}_{\mathrm{CP}} \cdot \mathbf{q} = 0$ and $\boldsymbol{\varepsilon}_{\mathrm{LP}} \cdot \mathbf{q} = 0$, respectively. For example, at a photon energy of $\omega = 1.55$ eV the TDCSs take the maximal value at the scattering and emitted angles of $\theta_s \sim 15.5^\circ$ and $\theta_e \sim -73^\circ$ (or $\theta_s \sim -15.5^\circ$ and $\theta_e \sim 73^\circ$) for the CP laser field and $\theta_s \sim 16.5^\circ$ and $\theta_e \sim -64^\circ$ (or $\theta_s \sim -16.5^\circ$ and $\theta_e \sim 64^\circ$) for the LP laser field.

For a different view of the density plots shown in Figs. 3(a) and 3(d) at a photon energy of 1.55 eV, we illustrate in Fig. 4 their corresponding three-dimensional graphs of TDCSs as a function of the polar angles θ_e and θ_s of the ejected and scattered electrons, for a CP field in Fig. 4(a) and a LP in Fig. 4(b), together with the field-free TDCS in Fig. 4(c).

In order to emphasize the importance of the atomic dressing as the photon energy increases, we display in Figs. 5(a)–5(f) results similar to those in Figs. 3(a)–3(f) but the direct and exchange atomic transition amplitudes $T^{(1)}_{N,\mathrm{d}}$ and

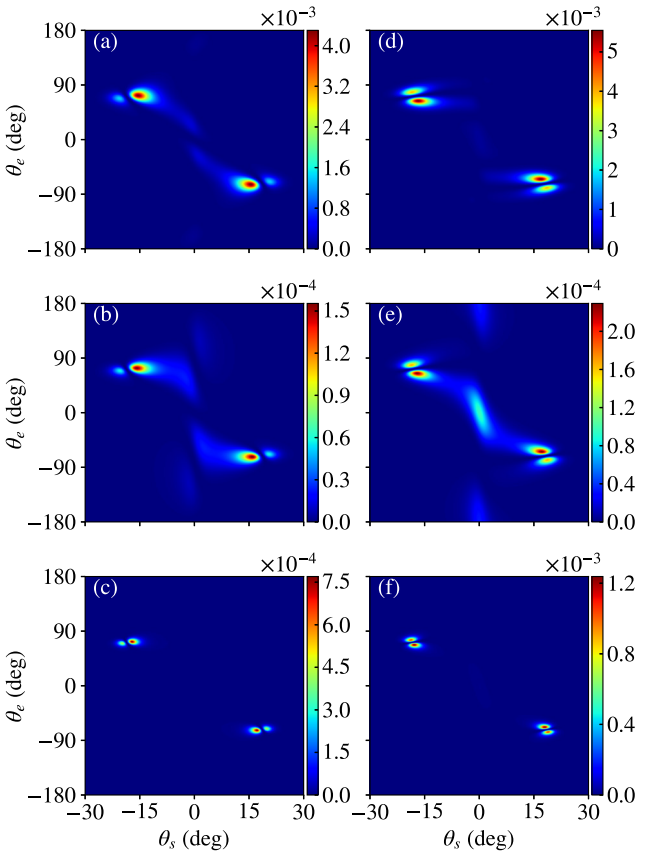

FIG. 3. TDCSs for the ionization of hydrogen by electron impact in the presence of a laser field, computed from Eq. (29), as a function of the ejected and scattered electron polar angles θ_e and θ_s, respectively, for one-photon absorption $N = 1$. The kinetic energies of the incident and ejected electrons are $E_i = 2$ keV and $E_e = 0.2$ keV, respectively, and the azimuthal angles are $\varphi_e = \varphi_s = 0^\circ$. The laser intensity is $I = 1\,\mathrm{TW\,cm^{-2}}$ and the photon energies are (a) and (d) $\omega = 1.55$ eV, (b) and (e) 4.65 eV, and (c) and (f) 9.3 eV. (a)–(c) Density plots of TDCSs calculated for the CP field with the polarization vector $\boldsymbol{\varepsilon}_{\mathrm{CP}} = (\mathbf{e}_x + i\mathbf{e}_y)/\sqrt{2}$. (d)–(f) Numerical results for the LP field with the polarization vector $\boldsymbol{\varepsilon}_{\mathrm{LP}} = \mathbf{e}_z$.

$T^{(1)}_{N,\mathrm{ex}}$ are ignored in the TDCS (29). We can glimpse the influence of the photon energy by looking first at the amplitude of the quiver motion α_0. A laser intensity of 1 $\mathrm{TW\,cm^{-2}}$ and a photon energy of 1.55 eV (Ti:sapphire laser) result in a quiver motion amplitude $\alpha_0 \sim 1.64$ a.u. and an argument of the Bessel function $X_{\mathrm{q}} \simeq 1.64|\boldsymbol{\varepsilon} \cdot \mathbf{q}|$, while for a larger photon energy of 4.65 eV (third harmonic of the Ti:sapphire laser) the corresponding amplitude α_0 and argument X_{q} are about nine times smaller. Hence, the magnitude of the TDCS peaks is about one order of magnitude smaller at a photon energy of 4.65 eV in Figs. 3(b) and 3(e) compared to Figs. 3(a) and 3(d) at 1.55 eV, while the electronic contribution in Figs. 5(b) and 5(e) is about two orders of magnitude smaller than that in Figs. 5(a) and 5(d). Moreover, at $\omega = 1.55$ eV, by comparing Figs. 3(a) and 3(d) with Figs. 5(a) and 5(d), we notice that the atomic dressing effects are small, since $T^{(1)}_{N=1,\mathrm{d(ex)}}/T^{(0)}_{N=1,\mathrm{d(ex)}} \simeq 4\omega/(1+q^2)$ as we have estimated in the LFA in Sec. II B, and therefore the electronic transition amplitudes give the

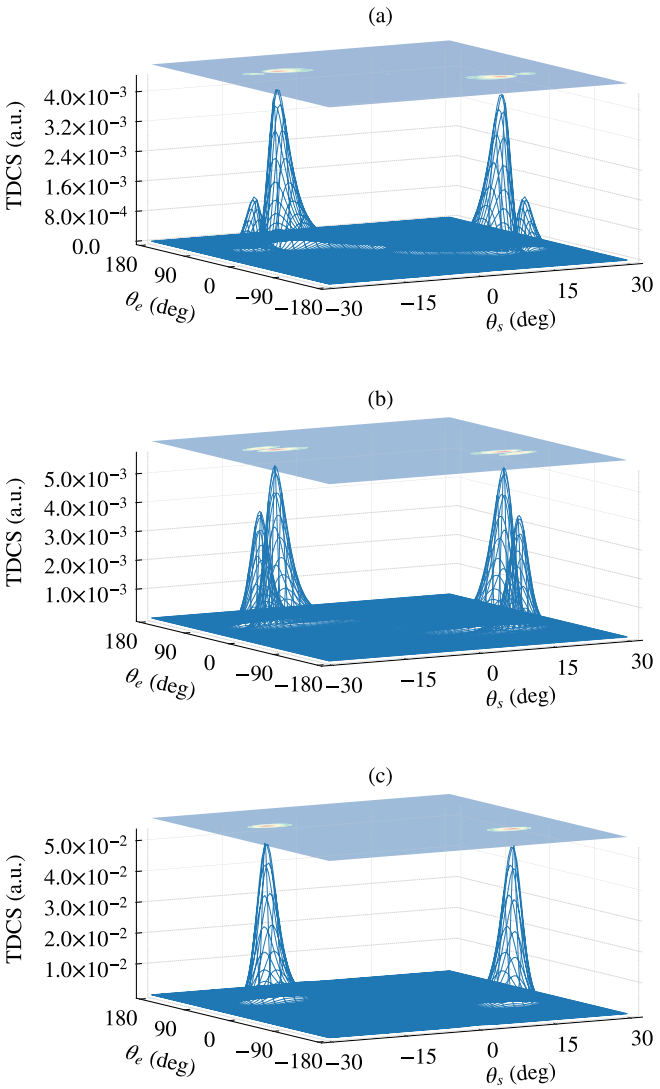

FIG. 4. Three-dimensional plots of the TDCSs presented in Figs. 3(a) and 3(d) at the photon energy $\omega = 1.55$ eV, as a function of the polar angles of the ejected and scattered electrons θ_e and θ_s, respectively, for (a) circular polarization and (b) linear polarization. (c) TDCS in the absence of the laser field.

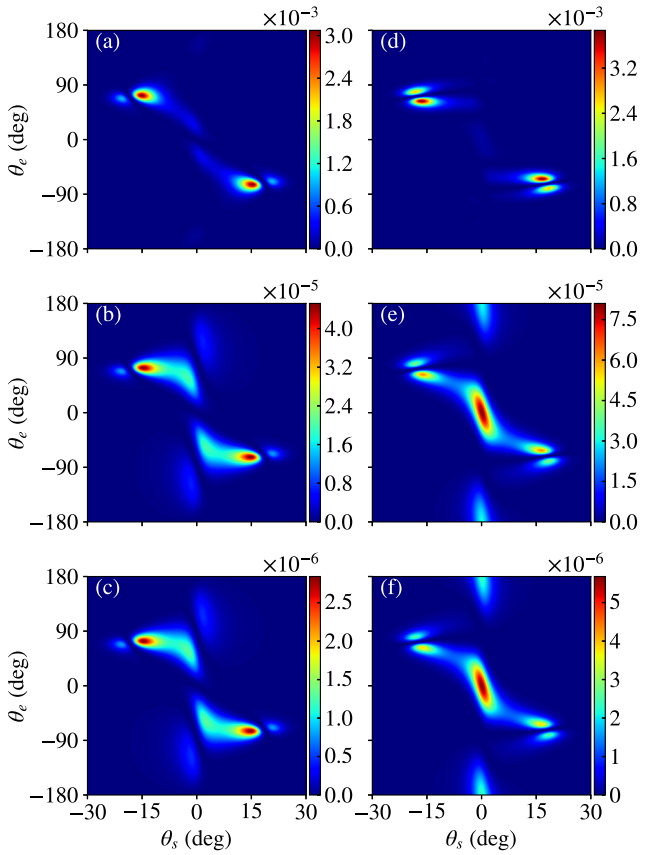

FIG. 5. Similar to Fig. 3, but only the electronic transition amplitudes $T_{N,\mathrm{d}}$ and $T_{N,\mathrm{ex}}$ are included in the calculation of the TDCS [Eq. (29)], while the atomic contributions are ignored.

largest contribution to the TDCS. In contrast, as the photon energy increases the atomic dressing effects increase and their contribution to the TDCS cannot be neglected. Here we may note that at forward scattering angles $\theta_e = 0^\circ$ and $\theta_s = 0^\circ$, we have $\boldsymbol{\varepsilon}_{\mathrm{CP}} \cdot \mathbf{q} = 0$ for the CP field and nonzero values for the LP field $\boldsymbol{\varepsilon}_{\mathrm{LP}} \cdot \mathbf{q} = k_i - k_s - k_e$. In addition, a strong atomic dressing effect is seen in the vicinity of the $1s - 2p$ resonance at a photon energy of 9.3 eV in Figs. 3(c) and 3(f), where the outgoing electrons are focused within narrow solid angles. Due to the vicinity of $1s - 2p$ excitation, the atomic transition amplitudes [Eqs. (18) and (23)] give a large contribution compared to the electronic transition amplitudes, as is shown in Figs. 5(c) and 5(f).

Now, since we are interested in the direction in which the maximum of the TDCS can be observed, we examine the TDCS at the scattered electron polar angle $\theta_s = 15^\circ$, which is close to the peaks of the TDCSs in Fig. 3, and vary the polar and azimuthal angles of the ejected electron, θ_e and φ_e. For simplicity, the azimuthal angle of the scattered electron is fixed at $\varphi_s = 0^\circ$. Thus, in Fig. 6 we illustrate TDCSs for the ionization of hydrogen by electron impact in the presence of a laser field as a function of the polar and azimuthal angles of the ejected electron at a photon energy $\omega = 4.65$ eV for one-photon absorption ($N = 1$) in Figs. 6(a) and 6(d), one-photon emission ($N = -1$) in Figs. 6(b) and 6(e), and no photon exchange ($N = 0$) in Figs. 6(c) and 6(f). In Figs. 6(a)–6(c) we show the density plots of TDCSs calculated for a CP laser field, while in Figs. 6(d)–6(f) we present the results for the LP case. In Fig. 7 we illustrate results similar to those in Fig. 6, but for a smaller scattering angle $\theta_s = 5^\circ$. The maximum values of TDCSs occur in the coplanar geometry around $\varphi_e = 180^\circ$, at the minimum values of q [Eq. (39)]. By comparing the TDCSs for LP laser fields in Figs. 6(a) and 6(d) with those in Figs. 6(d) and 6(e) for CP laser fields, there are noticeable differences between the numerical results, for both $N = 1$ and $N = -1$. As mentioned before, the condition $\boldsymbol{\varepsilon} \cdot \mathbf{q} \simeq 0$ is fulfilled at different polar angles for LP and CP laser fields. More specifically, a splitting of the TDCS peak is clearly noticeable for the LP field in Figs. 6(a) and 6(e), in the vicinity of $\theta_e \simeq 74.5^\circ$, where the condition $\boldsymbol{\varepsilon}_{\mathrm{LP}} \cdot \mathbf{q} \simeq 0$ is satisfied. In contrast, the splitting of the TDCS peak is barely visible for the CP field at $\theta_e \simeq 51^\circ$, in Figs. 6(a) and 6(b). Moreover, the maximum values of the TDCS occur at

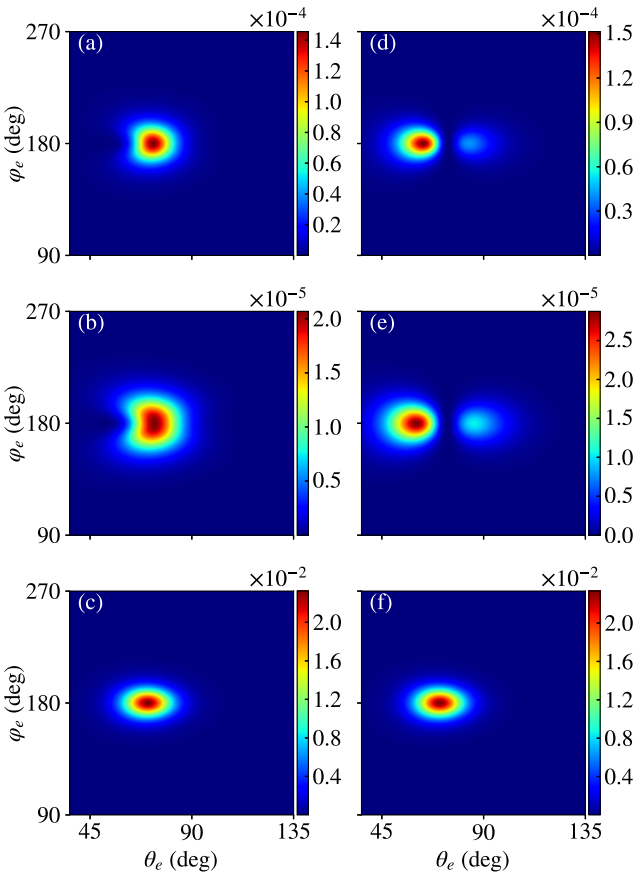

FIG. 6. TDCSs for the ionization of hydrogen by electron impact in the presence of a laser field, as a function of the polar and azimuthal angles of the ejected electron θ_e and φ_e, respectively, at photon energy $\omega = 4.65$ eV for (a) and (d) one-photon absorption ($N = 1$), (b) and (e) one-photon emission ($N = -1$), and (c) and (f) no photon exchange ($N = 0$). The polar and azimuthal angles of the scattered electron are $\theta_s = 15^\circ$ and $\varphi_s = 0^\circ$, respectively. (a)–(c) Density plots of TDCSs evaluated for a CP field. (d)–(f) Results for a LP field. The rest of the parameters regarding the scattering geometry, incident and outgoing electron kinetic energies, and laser intensity are the same as in Fig. 3.

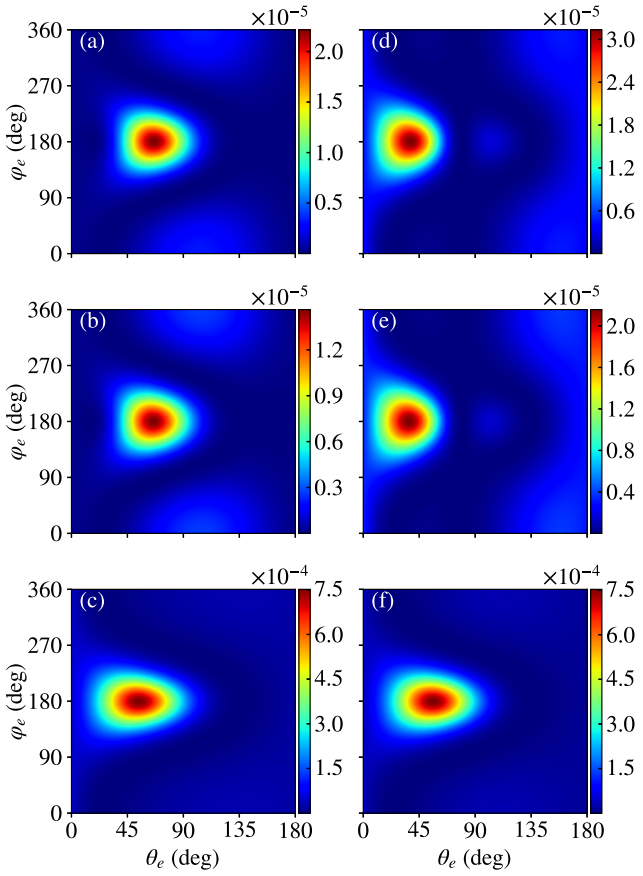

FIG. 7. Similar to Fig. 6, but the polar angle of the scattered electron is $\theta_s = 5^\circ$.

different values of the polar angle θ_e for CP compared to LP laser fields. However, the magnitude of TDCSs peaks by the CP laser field is comparable to that by the LP laser field.

The angular distributions of the TDCS for one-photon absorption compared to one-photon emission show similar features, but the one-photon absorption dominates the one-photon emission process as a result of the constructive ($N = 1$) and destructive ($N = -1$) interferences between the electronic and atomic contributions in the TDCS (29). We find that the ejected electron is observed with a high probability into a narrow cone in Fig. 6, while in Fig. 7 the ejected electron is emitted in a larger solid angle and the TDCS is almost one order of magnitude smaller. Specifically, in Fig. 6 at the scattering angle $\theta_s = 15^\circ$ the laser-assisted $(e, 2e)$ signal is focused in a narrow range of polar angles $60^\circ < \theta_e < 80^\circ$ for the CP field and $50^\circ < \theta_e < 70^\circ$ for the LP field, with the azimuthal angles $160^\circ < \varphi_e < 200^\circ$. In contrast, the TDCSs in Fig. 7 at the scattering angle $\theta_s = 5^\circ$ are focused in a wider range of both polar and azimuthal angles, namely, $40^\circ < \theta_e < 100^\circ$ for the CP field and $10^\circ < \theta_e < 70^\circ$ for the LP field, with $120^\circ < \varphi_e < 240^\circ$. Both TDCSs for CP and LP light at $\varphi_s = 0^\circ$ are symmetric with respect to reflection in the (x, z) plane, being invariant to the change $\varphi_e = \pi - \xi \to \pi + \xi$, with ξ an arbitrary angle. For no photon exchange ($N = 0$) in Figs. 6(c) and 6(f) and Figs. 7(c) and 7(f), the magnitude of the TDCS peak is about two orders of magnitude larger than those of the one-photon absorption or emission ($N = \pm 1$). The density plots of the laser-assisted TDCS by CP and LP laser fields at $N = 0$ are similar to the field-free case (not shown here) because at small X_q the laser field gives a negligible contribution to the ionization process.

In what follows let us consider in more detail the TDCS density plots for one-photon absorption ($N = 1$) presented in Figs. 6(a) and 7(a) for a CP laser field and in Figs. 6(d) and 7(d) for a LP laser field. Thus, in Fig. 8 we plot the numerical results for TDCSs, in logarithmic scale, for $\omega = 4.65$ eV and one-photon absorption at two scattering angles $\theta_s = 15^\circ$ in Fig. 8(a) and $\theta_s = 5^\circ$ in Fig. 8(b), with $\varphi_s = 180^\circ$ and $\varphi_e = 0^\circ$. The solid lines shows the TDCSs calculated for a CP laser field, the dashed lines presents the results for a LP laser field, and the dotted lines present the TDCSs in the absence of the laser field. In Fig. 8(a) the ejected electron is observed with a high probability in a narrow region, which is centered around the angles $\theta_e \sim 73^\circ$ (CP field) and $\theta_e \sim 63^\circ$ (LP field). We recall that the maximum values of the TDCS occur at

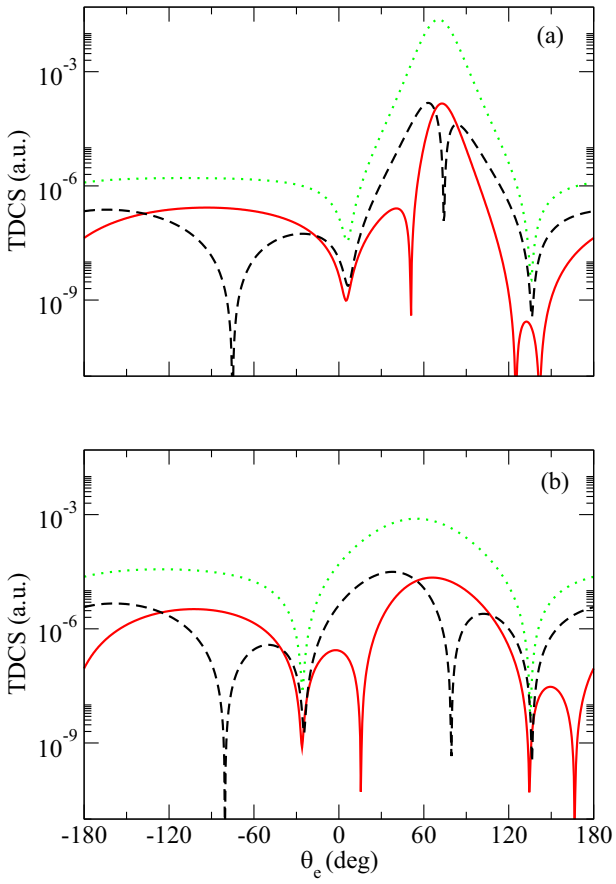

FIG. 8. Comparison of the TDCSs for ionization of hydrogen by electron impact in the presence of CP (solid lines) and LP (dashed lines) laser fields, in logarithmic scale, as a function of the polar angle of the ejected electron θ_e, for one-photon absorption ($N = 1$) at photon energy $\omega = 4.65$ eV and two different values of the scattered electron polar angle: (a) $\theta_s = 15^\circ$ and (b) $\theta_s = 5^\circ$. The dotted lines present the field-free TDCS. The azimuthal angles of the outgoing electrons are $\varphi_s = 180^\circ$ and $\varphi_e = 0^\circ$ and the rest of the parameters regarding the scattering geometry, incident and ejected electron kinetic energies, and laser intensity are the same as in Fig. 3.

specific combinations of polar and azimuthal angles $\theta_{e\,(s)}$ and $\varphi_{e\,(s)}$ which are determined by the minimum value of recoil momentum and are altered by the zeros of the argument of the Bessel functions X_q. The well-known effect of the laser is to decrease the magnitude of the TDCS peak which occurs at the minimum value of the residual ion momentum. Another effect of the laser field is the splitting of the TDCS peak by the kinematical minima whenever the scalar product $\boldsymbol{\varepsilon} \cdot \mathbf{q}$ becomes zero. Thus, the main peak of the TDCS is split by the CP laser field at $\theta_e \sim 51^\circ$ in Fig. 8(a), being symmetrically located with respect to the direction of the incident electron. For the LP case, the main peak is split by the laser field at $\theta_e \sim 74.5^\circ$, which is quite close to the minimum of the recoil momentum, and hence it will result in the specific angular distribution of the TDCS in Fig. 6(d).

In contrast, at $\theta_s = 5^\circ$ in Fig. 8(b) the electron is emitted into a larger solid angle and the main peak amplitude of the TDCSs is smaller than at $\theta_s = 15^\circ$, hence resulting in the specific angular distribution of TDCSs in Figs. 7(a) and

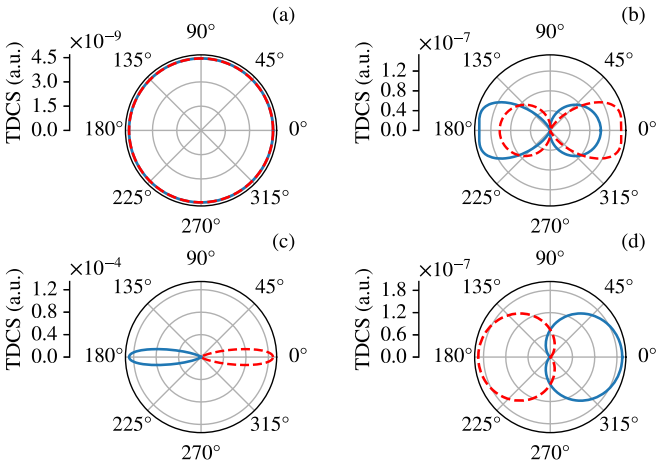

FIG. 9. TDCS for ionization of hydrogen by electron impact in the presence of a CP laser field as a function of the ejected electron azimuthal angle φ_e at photon energy $\omega = 4.65$ eV for one-photon absorption ($N = 1$) at four different values of the ejected electron polar angle θ_e: (a) 0°, (b) 30°, (c) 70°, and (d) 135°. The polar and azimuthal angles of the scattered electron are $\theta_s = 15^\circ$ and $\varphi_s = 0^\circ$, respectively, for the solid lines and $\varphi_s = 180^\circ$ for the dashed lines. The rest of the parameters concerning the scattering geometry, incident and ejected electron kinetic energies, and laser intensity are the same as in Fig. 3.

7(d). Both TDCSs for CP and LP laser fields are symmetric with respect to reflection and rotation in the (y, z) and (x, z) planes, namely, to the changes $\theta_e \to -\theta_e$ and $\varphi_e \to \pi + \varphi_e$, respectively. In Fig. 9 we illustrate the azimuthal distributions of the TDCS for ionization of hydrogen by electron impact in the presence of a CP laser field as a function of the ejected electron azimuthal angle φ_e at photon energy $\omega = 4.65$ eV for one-photon absorption, $N = 1$, at four different values of the ejected electron polar angle: $\theta_e = 0^\circ$ in Fig. 9(a), 30° in Fig. 9(b), 70° in Fig. 9(c), and 135° in Fig. 9(d). The polar angle of the scattered electron is $\theta_s = 15^\circ$, while the azimuthal angle is $\varphi_s = 0^\circ$ for the solid lines and $\varphi_s = 180^\circ$ for the dashed lines. In Fig. 10 we show results similar to

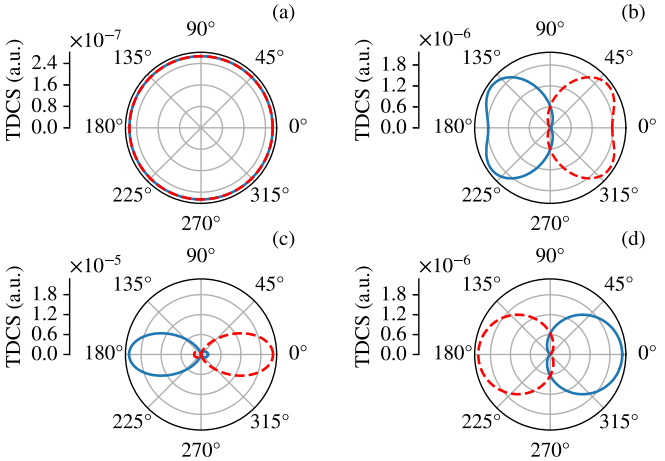

FIG. 10. Similar to Fig. 9, but the polar angle of the scattered electron is $\theta_s = 5^\circ$.

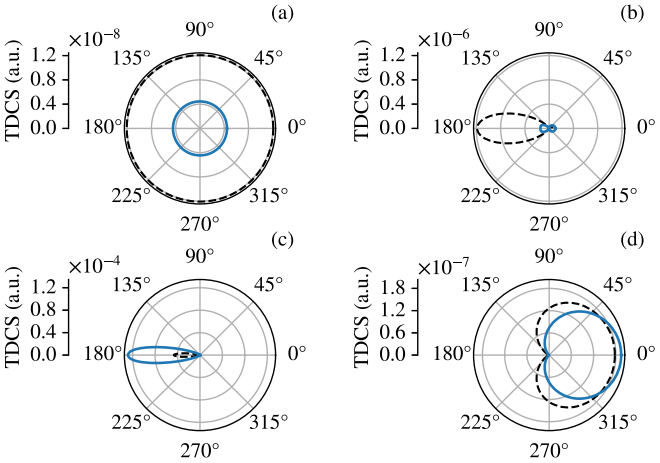

FIG. 11. Similar to Fig. 9, where the solid lines represent the results for a CP laser field and the dashed lines represent TDCSs for a LP laser field, at $\varphi_s = 0^\circ$.

those in Fig. 9, but the polar angle of the scattered electron is $\theta_s = 5^\circ$. For comparison, in Fig. 11 we show results of the laser-assisted TDCSs similar to those in Fig. 9 at $\theta_s = 15^\circ$, for both CP (solid lines) and LP (dashed lines) fields. The TDCS is symmetric with respect to reflection in the (x, z) plane, and at forward and backward polar angles $\theta_e = 0^\circ$ and 180°, respectively, the TDCS is independent of the azimuthal angle φ_e. At polar angles of the ejected electron close to the minimum of the recoil momentum, i.e., around $\theta_e \simeq 70^\circ$, the TDCS curves in Figs. 9(c) and 10(c) are quite deformed along the x axis (at $\varphi_e = 0^\circ$ and 180°), which explains the density plot distributions of TDCSs in Figs. 6(a) and 7(a). For azimuthal angles $\varphi_s \neq 0$ the TDCS is invariant to the change $\varphi_e = \pi + \varphi_s - \xi \to \pi + \varphi_s + \xi$, which implies a rotation with angle φ_s of the TDCSs in Fig. 9, as well a translation with φ_s of the TDCSs along the vertical axis in Figs. 6 and 7. The CP laser field can give larger TDCSs than in the LP case at the polar angles of the ejected electron situated in the vicinity of the kinematical minimum.

IV. CONCLUSION

To summarize, we have investigated the laser-assisted $(e, 2e)$ process (1) for fast electrons at moderate laser field intensities and we have analyzed the influence of the laser polarization in several numerical examples by comparing the TDCSs by CP and LP laser fields. An asymmetric noncoplanar scattering kinematics was considered in which the polar and azimuthal angles of the scattered electron are fixed, while those corresponding to the ejected electron are varied. We employed a semiperturbative method to derive the TDCS in the laser-assisted $(e, 2e)$ process in the first-order Born approximation in the scattering potential. For the interaction of the fast incoming and outgoing electrons with the laser field we used the nonperturbative Gordon-Volkov wave functions, while for the interaction of the H atom with the laser field we used the first-order TDPT [31]. The exchange terms between the outgoing electrons were included in the calculation of the TDCS. We also derived a simplified expression of the total TDCS at low values of the photon energy and low momentum of the residual ion. The TDCS was modified by the presence of the laser field and displayed a strong dependence on the directions of the ejected and scattered electrons.

Due to the Coulomb repulsion, the outgoing electrons were emitted and scattered in different half planes corresponding to polar angles with opposite signs. We showed that significant changes in the angular distributions of the TDCS could be predicted when using a CP laser field instead of a LP one. We established that by changing the laser polarization we could change the angular distributions of the ejected electron, and the peak magnitudes of TDCSs for circular polarization were lower when compared to those for linear polarization laser fields. The addition of the laser field changed the profile of the field-free TDCS, namely, the binary peaks were reduced in magnitude and split by the presence of the laser due to the kinematical minima which occur when $\boldsymbol{\varepsilon} \cdot \mathbf{q} = 0$, at different polar angles for CP and LP fields. We showed that at low photon energies the atomic dressing effects on the TDCS were small and the electronic transition amplitudes contributed the most, but the dressing effects increased in importance as the photon energy increased. We compared our numerical results with those published by Höhr *et al.* [21] for the He atom and we found reasonable qualitative agreement. In conclusion, our analytical formalism allows us to understand the physics of the laser-assisted $(e, 2e)$ process in a complementary way compared to the pure numerical calculations and provides supplementary information for theoretical and experimental investigations. The use of laser fields with circular polarization for the $(e, 2e)$ process can give larger TDCSs than in the LP case at the polar angles of the ejected electron in the vicinity of the kinematical minimum, when $\boldsymbol{\varepsilon}_{\mathrm{LP}} \cdot \mathbf{q} = 0$. Our findings demonstrate the strong influence of the laser polarization on the dynamics of laser-assisted $(e, 2e)$ process, and we hope that the theoretical results of this paper will provide valuable insights for experimental observation to predict more efficiently the optimal observation direction of the ejected electron.

ACKNOWLEDGMENTS

This research was supported by the Romanian Ministry of Research, Innovation and Digitalization under the Romanian National Core Program LAPLAS VII through Contract No. 30N/2023.

[1] F. Byron and C. Joachain, Phys. Rep. **179**, 211 (1989).

[2] $(e, 2e)$ *& Related Processes*, edited by C. T. Whelan, H. R. J. Walters, A. Lahmam-Bennani, and H. Ehrhardt, NATO Advanced Studies Institute, Series C: Mathematical and Physical Sciences (Springer Science+Business Media, Dordrecht, 1993), Vol. 414.

[3] *Coincidence Studies of Electron and Photon Impact Ionization*, edited by C. T. Whelan and H. R. J. Walters (Springer US, Boston, 1997).

[4] R. Camilloni, A. G. Guidoni, R. Tiribelli, and G. Stefani, Phys. Rev. Lett. **29**, 618 (1972).

[5] M. A. Coplan, J. H. Moore, and J. P. Doering, Rev. Mod. Phys. **66**, 985 (1994).

[6] E. Weigold and I. E. McCarthy, *Electron Momentum Spectroscopy* (Springer US, Boston, 1999).

[7] V. G. Neudachin, Y. V. Popov, and Y. F. Smirnov, Phys. Usp. **42**, 1017 (1999).

[8] F. Ehlotzky, A. Jaroń, and J. Kamiński, Phys. Rep. **297**, 63 (1998).

[9] M. Jain and N. Tzoar, Phys. Rev. A **18**, 538 (1978).

[10] P. Cavaliere, G. Ferrante, and C. Leone, J. Phys. B **13**, 4495 (1980).

[11] P. Cavaliere, C. Leone, R. Zangara, and G. Ferrante, Phys. Rev. A **24**, 910 (1981).

[12] A. Chattopadhyay and C. Sinha, Phys. Rev. A **72**, 053406 (2005).

[13] F. W. Byron Jr. and C. J. Joachain, J. Phys. B **17**, L295 (1984).

[14] C. J. Joachain, P. Francken, A. Maquet, P. Martin, and V. Veniard, Phys. Rev. Lett. **61**, 165 (1988).

[15] D. B. Milošević and F. Ehlotzky, Phys. Rev. A **56**, 3879 (1997).

[16] R. Taïeb, V. Véniard, A. Maquet, S. Vucic, and R. M. Potvliege, J. Phys. B **24**, 3229 (1991).

[17] A. Makhoute, D. Khalil, A. Maquet, C. J. Joachain, and R. Taïeb, J. Phys. B **32**, 3255 (1999).

[18] K. A. Kouzakov, Y. V. Popov, and M. Takahashi, Phys. Rev. A **82**, 023410 (2010).

[19] A. A. Bulychev, K. A. Kouzakov, and Y. V. Popov, Phys. Lett. A **376**, 484 (2012).

[20] C. Höhr, A. Dorn, B. Najjari, D. Fischer, C. D. Schröter, and J. Ullrich, Phys. Rev. Lett. **94**, 153201 (2005).

[21] C. Höhr, A. Dorn, B. Najjari, D. Fischer, C. Schröter, and J. Ullrich, J. Electron Spectrosc. Relat. Phenom. **161**, 172 (2007).

[22] T. Hiroi, Y. Morimoto, R. Kanya, and K. Yamanouchi, Phys. Rev. A **104**, 062812 (2021).

[23] G. Buică, Phys. Rev. A **106**, 022804 (2022).

[24] W. Gordon, Z. Phys. **40**, 117 (1926).

[25] D. M. Wolkow, Z. Phys. **94**, 250 (1935).

[26] B. H. Bransden and C. J. Joachain, *Physics of Atoms and Molecules* (Longman, Harlow, 1983).

[27] C. J. Joachain, N. J. Kylstra, and R. M. Potvliege, *Atoms in Intense Laser Fields* (Cambridge University Press, Cambridge, 2011).

[28] L. V. Keldysh, J. Exp. Theoret. Phys. **47**, 1945 (1964) [Sov. Phys. JETP **20**, 1307 (1965)].

[29] F. H. M. Faisal, J. Phys. B **6**, L89 (1973).

[30] H. R. Reiss, Phys. Rev. A **22**, 1786 (1980).

[31] V. Florescu and T. Marian, Phys. Rev. A **34**, 4641 (1986).

[32] N. F. Mott and H. S. W. Massey, *The Theory of Atomic Collisions* (Oxford University Press, Oxford, 1965).

[33] C. J. Joachain, *Quantum Collision Theory*, 3rd ed. (North-Holland, Amsterdam, 1983).

[34] B. Lohmann and E. Weigold, Phys. Lett. **86A**, 139 (1981).

[35] C. Leone, S. Bivona, R. Burlon, F. Morales, and G. Ferrante, Phys. Rev. A **40**, 1828 (1989).

[36] Y. Attaourti and S. Taj, Phys. Rev. A **69**, 063411 (2004).

[37] J. Zhang and T. Nakajima, Phys. Rev. A **75**, 043403 (2007).

[38] T. A. Marian, Phys. Rev. A **56**, 3988 (1997).

[39] G. Buica, Phys. Rev. A **96**, 043419 (2017).

[40] G. Buica, Phys. Rev. A **98**, 053427 (2018).

[41] E. Weigold, C. J. Noble, S. T. Hood, and I. Fuss, J. Phys. B **12**, 291 (1979).

[42] A. Cionga, F. Ehlotzky, and G. Zloh, Phys. Rev. A **62**, 063406 (2000).

[43] A. Cionga, F. Ehlotzky, and G. Zloh, J. Phys. B **33**, 4939 (2000).

[44] G. Buica, Phys. Rev. A **92**, 033421 (2015).

[45] G. Buică, J. Quant. Spectrosc. Radiat. Transfer **187**, 190 (2017).

[46] G. Buică, Phys. Rev. A **108**, 059901(E) (2023).

[47] A. Dubois, A. Maquet, and S. Jetzke, Phys. Rev. A **34**, 1888 (1986).

[48] A. Cionga, F. Ehlotzky, and G. Zloh, Phys. Rev. A **61**, 063417 (2000).

[49] A. Dubois and A. Maquet, Phys. Rev. A **40**, 4288 (1989).

[50] A. Cionga and G. Zloh, Laser Phys. **9**, 69 (1999).

[51] A. Cionga and V. Florescu, Phys. Rev. A **45**, 5282 (1992).

[52] G. Shchedrin and A. Volberg, J. Phys. A: Math. Theor. **44**, 245301 (2011).

[53] V. I. Ochkur, J. Exp. Theoret. Phys. **47**, 1746 (1964) [Sov. Phys. JETP **20**, 1175 (1965)].

[54] G. Watson, *A Treatise on the Theory of Bessel Functions* (Cambridge University Press, Cambridge, 1995).

[55] N. M. Kroll and K. M. Watson, Phys. Rev. A **8**, 804 (1973).